Novel Imaging Techniques for Heart Failure

Josep L Melero-Ferrer, Raquel López-Vilella, Herminio Morillas-Climent, Jorge Sanz-Sánchez, Ignacio J Sánchez-Lázaro, Luis Almenar-Bonet and Luis Martínez-Dolz

Advanced Heart Failure and Heart Transplantation Unit, Cardiology Department, Hospital Universitari i Politècnic La Fe, Valencia, Spain

Abstract

Imaging techniques play a main role in heart failure (HF) diagnosis, assessment of aetiology and treatment guidance. Echocardiography is the method of choice for its availability, cost and it provides most of the information required for the management and follow up of HF patients. Other non-invasive cardiac imaging modalities, such as cardiovascular magnetic resonance (CMR), nuclear imaging-positron emission tomography (PET) and single-photon emission computed tomography (SPECT) and computed tomography (CT) could provide additional aetiological, prognostic and therapeutic information, especially in selected populations. This article reviews current indications and possible future applications of imaging modalities to improve the management of HF patients.

Keywords

Heart failure, imaging, ecocardiography, computed tomography, cardiac magnetic resonance, nuclear imaging

Disclosure: The authors have no conflicts of interest to declare.
Received: 9 December 2015 **Accepted:** 21 January 2016 **Citation:** *Cardiac Failure Review*, 2016;**2**(1):27–34 DOI: 10.15420/cfr.2015:29:2
Correspondence: Josep L Melero, Advanced Heart Failure and Heart Transplantation Unit, Cardiology Department, Hospital Universitari i Politècnic La Fe, Avenida Abril Martorell 106, 46026 Valencia, Spain. E: josep.melero@gmail.com

Heart failure (HF) is an epidemic with an increasing prevalence and an absolute mortality rate of approximately 50 % within 5 years of diagnosis. Imaging plays a main role in HF diagnosis, assessment of aetiology and treatment guidance. This article reviews current HF applications for all the available non-invasive imaging modalities: echocardiography, cardiovascular magnetic resonance (CMR), nuclear imaging-positron emission tomography (PET) and single-photon emission computed tomography (SPECT) and computed tomography (CT). Echocardiography, with its recent developments, such as 3D echo, is the main imaging test used in the evaluation of HF patients, given its availability and reliability in assessing cardiac structure and function. CMR allows the characterisation of myocardial tissue, in addition to providing information on the structure and cardiac function, so it is a great help in the determination of HF aetiology and may predict patient outcomes. Nuclear imaging can detect ischaemia and viability and can obtain additional prognostic data. Cardiac CT is a reliable method for the detection of coronary artery disease (CAD), and recent advances have in turn provided information about function and myocardial perfusion. In general, available imaging methods yield reliable measures of cardiac performance in HF, and recent advances allow detection of subclinical disease. In the following pages, current indications and possible future applications of each one of the above mentioned modalities are developed with further detail.

Echocardiography

Although echocardiography is a relatively 'ancient' technique, its versatility makes it unique in the provision of volumes, function, haemodynamics or valvular regurgitation. In addition, because of its availability, safety and low cost, echocardiography is the first and most widely used test for the diagnosis, selection of appropriate treatment and prognosis of HF.[1] Echocardiography is also the most used imaging method in the reassessment of HF patients. It remains unclear when to repeat echocardiographic exams, but it is deemed appropriate at least in patients with worsening symptoms.

Systolic Function

Global left ventricular (LV) function is of paramount importance regarding therapeutic decisions. Visual estimation of ejection fraction (EF), the Teichholz and Simpson methods, have been widely validated.[2,3] However, in 2D imaging, because of its operator-dependent nature, repeated testing has a high probability of producing variable volume and EF results.

The apparition of 3D fully sampled matrix transthoracic echocardiography has enabled easier acquisition of images,[4] simplifying its routinary application. There have been many studies comparing 2D and 3D echocardiography (2DE and 3DE) and a 'reference' standard (generally CMR). A recent meta-analysis of all 3DE studies evaluating LV volumes and EF demonstrated that 3DE generally underestimated volumes, but not as significantly as 2DE. There was also less variability than 2D compared with CMR.[5] Nonetheless, 3DE echocardiography may be challenging and not practical in patients with low image quality (e.g. critical patients), in whom 2DE measures are more realiable. 3DE is also a less standardised techique than 2DE, and because of this reason most laboratories use the more universally applicable 2DE measurements in clinical practice. Only recently, large analyses of LV parameters using 3DE in large cohorts of healthy individuals have been published to establish race, age and gender-specific reference ranges to facilitate the standardisation of this technique.[6]

The most commonly used strain-based measure of LV global systolic function is global longitudinal strain (GLS), which is usually assessed by

Figure 1: Novel Techniques in Echocardiography Applied on Heart Failure Patients

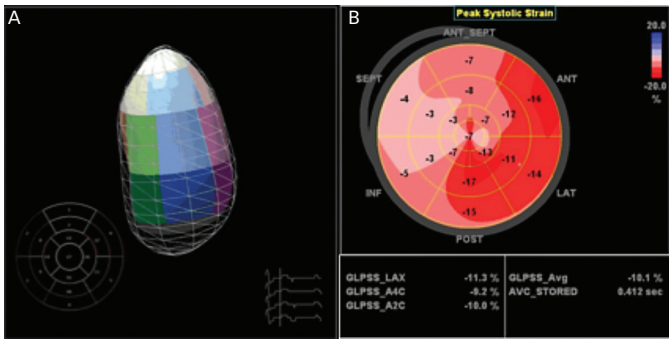

(A) 3D echo displaying endocardial surface rendering of the left ventricle. (B) Bulls-eye plot of regional strain of a patient with ischaemic cardiomyopathy. Scar (septal wall) and ischaemic (anteroseptal and inferior walls) tissues show lower global longitudinal strain (GLS) values than healthy tissue (lateral wall)

Figure 2: Example of Left Ventricular Dyssynchrony Analysis from Mid-ventricular Short-axis Views in a Patient With Left Bundle Branch Block

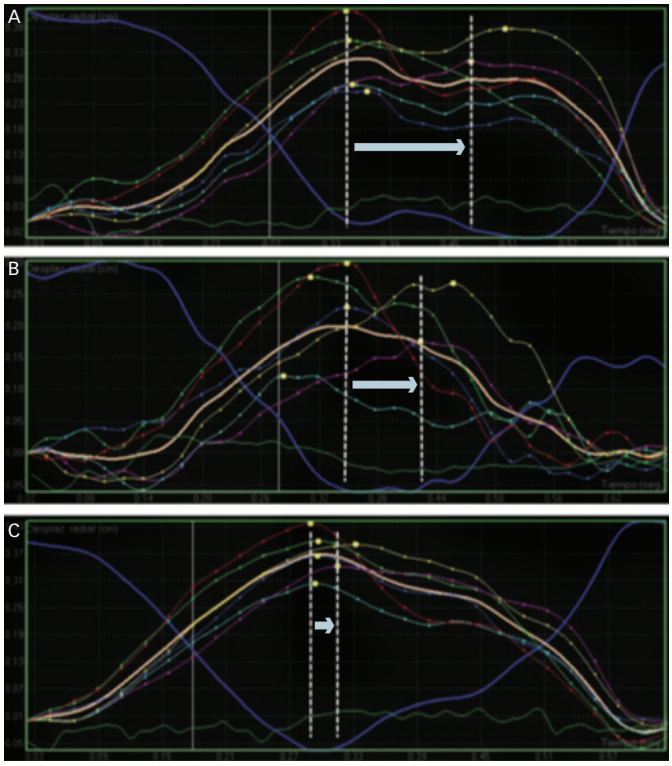

Dyssynchrony is shown as time difference (white arrow) between time-to-peak speckle-tracking radial strain in anterior septum (red curve) and posterior wall peak speckle-tracking strain (purple curve). (A) In baseline conditions, this patient exhibited significant left ventricular (LV) dyssynchrony (QRS width 175 ms). Furthermore, there was a delayed mechanical activation of the posterior wall compared with the anteroseptum (AS-P delay 134 ms). (B) With conventional biventricular pacing configuration, a decrease in the value of LV dyssynchrony was showed (AP-S delay 80 ms). (C) With multi-point pacing configuration, a higher decrease in LV dyssynchrony was shown (AS-P delay 34 ms) by earlier mechanical activation of the posterior wall that is synchronised to the timing of mechanical activation of the anteroseptal wall.

speckle-tracking echocardiography and describes the relative length change of the LV myocardium between end-diastole and end-systole. The preponderance of currently available data is for midwall GLS, and, although there is a wide heterogeneity in the published literature, a peak GLS in the range of 20 % can be expected in a healthy person.[7,8] It is essential to know the pitfalls and limitations of this method, specially the critical importance of optimised echocardiographic recordings and avoidance of apical foreshortening (which may significantly change the value of the obtained measurements).

Strain is of special interest in two clinical scenarios. Studies in patients with chemotherapy demonstrate that early alterations of myocardial deformation precede significant change in EF. A 10 % to 15 % early reduction in GLS during therapy is the most useful parameter for the prediction of cardiotoxicity, defined as a drop in LVEF or HF.[9] Moreover, 2D speckle-tracking imaging could be useful in differentiating cardiac amyloidosis from other causes of LV hypertrophy by showing reduced basal strain and regional variations in LS from base to apex and a relative 'apical sparing' (average apical LS/[average basal LS + mid-LS]) pattern. GLS also provided incremental prognostic value over N-terminal of the prohormone brain natriuretic peptide (NT-proBNP), cardiac troponin and other clinical variables.[10,11] In addition, although currently at an experimental level, strain imaging may help to detect subclinical cardiac dysfunction, e.g. in patients with diabetes.

Diastolic Function

Comprehensive diastolic assessment by tissue Doppler imaging, transmitral flow velocities and deceleration time, pulmonary venous Doppler, left atrial (LA) size and pulmonary artery pressures is mandatory in the evaluation of suspected HF. Nonetheless, the concordance between observers in this setting is limited.[12]

LA volume has a stronger association with outcomes compared with anteroposterior diameter. 3DE is more accurate than 2D assessment and provides fewer underestimated values in connection with CMR.[13]

In some patients, LV diastolic pressures are normal at rest but become abnormal under exercise. The typical echocardiographic parameters acquired during exercise or immediately thereafter are the E/e' ratio and peak tricuspid regurgitant velocity.[14] These parameters have a high specificity (96 %) but a relatively low sensitivity (76 %). An increase in the E/e´ ratio under physical exercise indicates a concomitant increase in LV end-diastolic pressures and a worse prognosis.[15,16]

Strain rate during the isovolumetric relaxation time (IVRsr) or early diastolic strain rate (e´sr), derived from global longitudinal speckle-tracking strain, were recently proposed to estimate LV filling pressures, although both parameters are still experimental.[17]

Right Ventricular Function

Pulmonary artery systolic pressure and TAPSE represent the minimum dataset of RV parameters in HF patients.[18] Other common techniques used are DTI derived s´ wave velocity, fractional area change and Tei index (which also evaluates diastolic function).

One emergent technique is RV 3D EF, which does not require geometric assumptions. Real-time 3D techniques have been shown to accurately provide objective measurement of RV volumes[19] and are especially attractive after cardiac surgery, when conventional indices of longitudinal RV function are generally reduced.[20]

Strain, particularly speckle tracking technique of the free wall, is a promising technique. Although less validated than in the LV, pooled data suggest that global longitudinal RV free wall strain lower than -20 % is likely abnormal. This parameter has prognostic value in advanced chronic HF.[21,22]

Aetiology of Heart Failure

Echocardiography is inferior compared with other imaging methods (e.g. CMR) in determining the aetiology of HF. However, stress

echocardiography can rule out ischaemia (with experimental techniques such as the use of microbubbles in development),[23] and is of special interest because of its dynamic nature, in doubtful cases of hypertrophic cardiomyopathy or mitral regurgitation.[24,25] Moreover, 3D echocardiography can help to elucidate the exact mechanism of some underlying valvulopathies, e.g. mitral valve prolapse.

Selection and Optimisation of Therapies

Echocardiography has been exhaustively evaluated in cardiac resynchronisation therapy (CRT), and some signs, e.g. septal flash, seem to indicate higher likelihood of success. Although dyssynchrony failed to improve patient selection beyond electrocardiogram (ECG) criteria,[26] newer methods such as speckle tracking and 3D echocardiography are under investigation. By contrast, radial strain demonstrated its value in guiding the placement of the LV lead and subsequently improving the response to CRT in the small trials Targeted Left Ventricular Lead Placement to Guide Cardiac Resynchronization Therapy (TARGET) and A Prospective Randomized Controlled Study of Echocardiographic-Guided Lead Placement For Cardiac Resynchronization Therapy (STARTER).[27] Nowadays, no accepted echo criteria for CRT implantation exist, and it is still an experimental field.

Echocardiography also has a main role in the selection and follow-up of patients with LV assist devices, with routine exams recommended to optimise the performance of these devices.[28]

Cardiovascular Magnetic Resonance

The high spatial and temporal resolution of CMR makes it suitable for use in the assessment of right (RV) and LV, providing a comprehensive study that includes anatomical evaluation, functional data and great information about myocardial perfusion and viability.[29]

During a CMR examination, the patient is brought into a high-strength static magnetic field that aligns the spins of the hydrogen atoms. These atoms are then excited intermittently by pulses of radiofrequency waves (MR sequences) and the signal emitted from the body in return is detected, determining two distinct MR relaxation parameters, longitudinal relaxation time (T1) and transverse relaxation time (T2). A CMR sequence consists of a series of radiofrequency pulses, magnetic gradient field switches and timed data acquisitions. To prevent artifacts from cardiac motion, most CMR images are generated with fast sequences gated to the R-wave of the ECG. Respiratory motion, another source of artifacts, is usually eliminated by acquiring CMR images in end-expiratory breath-hold.

Late gadolinium enhancement (LGE) patterns have been shown to provide diagnostic utility for distinguishing between ischaemic cardiomyopathy (ICM) and non-ischaemic cardiomyopathy (NICM),[30] but gadolinium-based contrast agents (GBCA) have been recently linked with a rare multisystemic fibrosing disorder known as nephrogenic systemic fibrosis. The patients at risk of developing this disease are those with severe renal insufficiency (glomerular filtration rate <30 ml/min/1.73 m^2), there is no specific treatment and symptoms may appear from several days to few years after the exposition. Therefore, in high-risk patients, GBCA should be avoided unless the diagnostic information is essential and not available from non-contrast enhanced CMR or other imaging modalities

Ischaemia Assessment

CMR, and in particular the LGE and T2-weighted ('edema') imaging, is useful to determine whether a LV dysfunction has an ischaemic aetiology.[31,32]

Figure 3: Examples of Late Gadolinium Enhancement Patterns (Arrows)

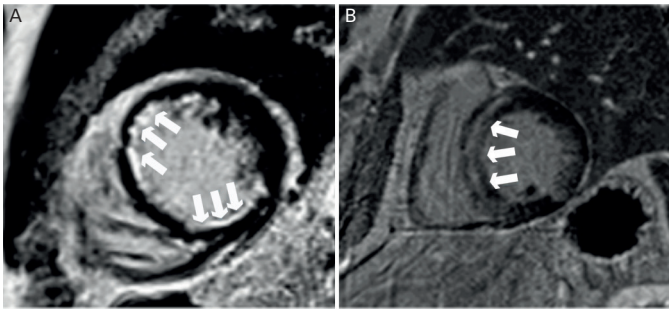

Dyssynchrony is shown as time difference (white arrow) between time-to-peak speckle-tracking radial strain in anterior septum (red curve) and posterior wall peak speckle-tracking strain (purple curve). (A) In baseline conditions, this patient exhibited significant left ventricular (LV) dyssynchrony (QRS width 175 ms). Furthermore, there was a delayed mechanical activation of the posterior wall compared with the anteroseptum (AS-P delay 134 ms). (B) With conventional biventricular pacing configuration, a decrease in the value of LV dyssynchrony was showed (AP-S delay 80 ms). (C) With multi-point pacing configuration, a higher decrease in LV dyssynchrony was shown (AS-P delay 34 ms) by earlier mechanical activation of the posterior wall that is synchronised to the timing of mechanical activation of the anteroseptal wall.

Figure 4: Iodine-123-metaiodobenzylguanidine Imaging in Heart Failure

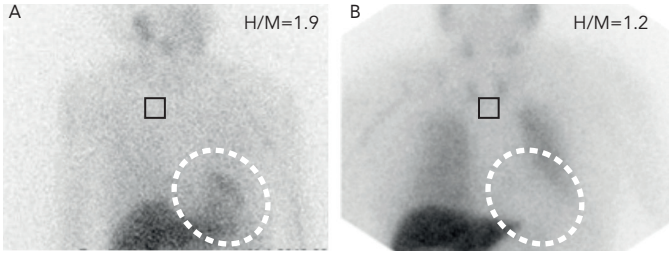

Uptake reduction with the progression of the severity of the disease. (A) Patient with heart failure (HF) in functional class II. (B). Patient with HF in functional class IV. H/M = heart to mediastinal ratio.

Figure 5: Contrast-enhanced Multidetector Computed Tomography Image

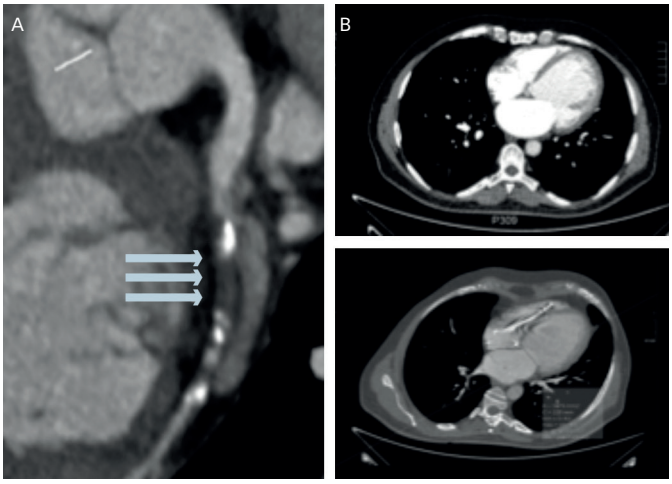

(A) Coronary computed tomography (CT) showing significant stenosis on circumflex artery. (B). Thoracic CT with helical acquisition after administration of intravenous iodinated contrast. Reconstructions of 2 mm, filter mediastinum and lung. Severe dilation of left cavities (left ventricle basal diameter of 76 mm, left atrium area of 34 cm2). Right cavities not dilated. Cardiac resynchronisation therapy device, distal end of electrodes in right ventricle apex, right atrial appendage and left marginal vein.

A recent study on the diagnostic utility of CMR found 100 % sensitivity and 96 % specificity for the identification of the cardiomyopathy aetiology,[33] reducing requirements of invasive angiography. However, total

absence of LGE does not completely rule out ischaemic cardiomyopathy in the rare setting of global myocardial hibernation.

The typical LGE in ICM should always involve the subendocardium (subendocardial or transmural) and be located in a region that is consistent with the perfusion territory of an epicardial coronary artery.[34] Between 10 % and 26 % of NICM patients without features of infarction show patchy or longitudinal striae of midwall hyperenhancement unrelated to a particular coronary artery territory, this distinct pattern of LGE corresponds to focal fibrosis.[35]

Stress perfusion CMR accurately identifies significant CAD, with higher accuracy than SPECT perfusion imaging.[36] In HF patients, CMR has shown an excellent safety profile when assessing ischaemia or viability.[37]

Viability Assessment

Multiple studies have confirmed the ability of LGE-CMR to predict recovery of contractile function after revascularisation.[38,39] Despite the contradictory findings of the Surgical Treatment for Ischemic Heart Failure (STICH) viability trial,[40] a more recent study has shown that the identification of viable but dysfunctional myocardium using LGE-CMR in HF patients is associated with worse outcomes when managed medically rather than undergo surgical revascularisation.[41]

Scars taking up >75 % of wall thickness indicate that the likelihood for functional recovery is low, but scars <25 % have a positive predictive accuracy of functional improvement.[42] The predictive value of segments with an intermediate (25 % to 75 %) transmural extent of scarring is lower. In these situations, a low-dose dobutamine study to assess the contractile reserve may be helpful.

A considerable number of patients (5–50 %) show lack of restoration of blood flow at myocardial level despite a successful procedure. This is called no-reflow and is due to microvascular obstruction.[43] It is related to more severe myocardial damage, increases with the duration of ischaemia time and is independently associated with lack of functional recovery, adverse ventricular remodelling and worse patient outcome.[44,45] It typically presents on LGE imaging as a subendocardially located hypointense area within the enhanced myocardium.

Therapy Guidance

The scar extent and the spatial distribution of LGE have been proposed as predictors of response in HF patients referred for CRT.[46,47] Those patients with transmural necrosis in either the septal or inferolateral walls experience an absence of improvement in LV volumes at 6 months. Performance of LGE-CMR prior to CRT implantation can help to guide the procedure; therefore, the lead can be delivered to viable tissue targets, improving event-free survival.[48]

In the same way, LGE-CMR can also predict arrhythmia risk. Among patients with ICM or NICM, those having appropriate ICD therapy or who had survived sudden cardiac death (SCD) showed higher scar extent on LGE imaging.[49]

Diffuse Fibrosis Assessment

One of the most promising future applications of CMR is the ability to identify diffuse myocardial collagen content. This approach could be useful to detect subclinical disease in at-risk populations, such as hypertensive or diabetic patients, infiltrative myocardial diseases, etc. This technique is based in T1 mapping of pixel-based quantifications of gadolinium retention.[50]

Cardiovascular Magnetic Resonance in Other Cardiomyopathies

Acute myocarditis may present as new-onset HF and its diagnosis could be challenging. The T2-weighted images show hyperintense subepicardial and midwall areas of myocardial oedema.[51] LGE is typically seen more pronounced in the subepicardial areas in inferolateral segments. Finally, hyperaemia and capillary leak (visualised on CMR images acquired early after gadolinium injection) have shown to be the best predictor in patients with chronic myocarditis.[52]

Regarding hyperthrophic cardiomyopathy, LGE extent is an independent predictor of adverse outcome.[53,54] In cardiac amyloidosis, LGE characteristically involves the subendocardium in a circumferential pattern, showing sometimes a patchier transmural pattern.[55]

Nuclear Imaging

Nowadays, the main clinical application for radionuclide imaging in HF is myocardial perfusion imaging for the assessment of ischaemia and/or viability.[56] The evaluation of sympathetic innervation by SPECT or PET has regained interest in the last years due to the apparition of new articles regarding its prognostic and predictive value.

Myocardial Blood Flow and Viability Testing

One of the first steps when studying a patient with HF is the identification of the underlying aetiology. Moreover, those patients with ICM and viable myocardium could benefit from revascularisation procedures, as some dysfunctional myocardium may not be irreversibly damaged. Nuclear imaging could be useful in this setting.

SPECT imaging with thallium-201 (201Tl) or technetium 99m (99mTc) has shown remarkable diagnostic capabilities to evaluate for the presence of infarction, ischaemia and/or viability.[56] Prior studies suggest excellent negative predictive values but poor positive negative values.[57] Reversible perfusion defects indicate ischaemia and fixed defects indicate scarring tissue. In general, ICM shows more extensive, diffuse and severe perfusion defects than NICM, but a noteworthy degree of overlap exists. Gated SPECT improves accuracy and provides information on LV volumes, LVEF and motion abnormalities.[58] Summed scores can be derived from this technique. Higher summed stress scores were found in patients with ICM.[58] SPECT perfusion defects also predict mortality in patients with ICM.[59,60]

PET imaging can also be used for this purpose. This technique determines an absolute quantification of myocardial blood flow and coronary flow reserve (CFR), as well as providing higher temporal and spatial resolution. For this reason, PET has better diagnostic performance than SPECT to detect ICM.[61] In addition, PET myocardial perfusion reserve has shown[61] to be a stronger predictor of unfavourable outcomes in ICM. Likewise, in NICM, CFR abnormalities can be detected due to microvasculature disease[62] and have been associated with increased risk of death.[63]

Radionuclide techniques are of use also to evaluate the presence of viable myocardium in patients with ICM. SPECT has been widely utilised in this scope, demonstrating high sensitivity to detect viability.[64,65] Nevertheless, the gold standard for myocardium viability assessing is 18-fludeoxyglucose (18F-FDG) PET. Metabolic

Table 1: Main Indications and Applications for Each one of the Available Imaging Modalities in the Assessment of Heart Failure Patients

	2D ECO	3DE	Strain	Cardiovascular Magnetic Resonance	Nuclear	Computed Tomography
LV/RV volumes	RU	AI		AI (GS)		AI
LV systolic function	RU	AI	AI	AI (GS)		
LV diastolic function	RU (GS)		AI	AI		
RV function	RU	AI	AI	AI (GS)		
Ischaemia	RU		AI	AI (GS)	AI (GS)	
Viability	RU		AI	AI (GS)	AI (GS)	
Cardiomyopathies and other heart failure aetiologies	RU		AI	AI (GS)		AI
Risk assessment (arrhythmia)						
Therapy guidance (cardiac resynchronisation therapy)						
Follow-up	RU					

Green: best performance of the technique for this indication; yellow: the technique could provide useful information for this indication; red: no/little use for this indication. AI = provides additional information to that obtained with 2D echocardiogram; GS = gold standard; RU = routinely used for this indication. LV = left ventricular; RV = right ventricular.

PET imaging yields the highest accuracy (>90 % sensitivity) for predicting functional recovery[66] after revascularisation. Data obtained from the PET and Recovery Following Revascularization-2 (PARR-2) study[67] showed a threshold of 7 % of hibernating myocardium above which a patient could benefit from revascularisation. Although there is considerable evidence in the literature[68] proving improved survival with revascularisation in patients with viable myocardium, surprisingly, the STICH study[40] failed to find a correlation between demonstrations of myocardial viability and benefit from revascularisation.

Sympathetic Activity

Hyperactivity of the autonomic nervous system (ANS) plays a major role in the pathophysiology of HF, causing myocardial β-adrenoceptor down-regulation. Viable myocardium with reduced innervation may be hyperresponsive to catecholamines, leading to the development of ventricular tachycardia (VT). There are SPECT/PET tracers that are analogues of the sympathetic neurotransmitters.[69] As they are uptaken and stored in the presynaptic nerve endings, the visualisation of sympathetic innervation is warranted. SPECT imaging with iodine-123-metaiodobenzylguanidine (123I-MIBG) is the most often used. 123I-MIBG studies comprise both planar and SPECT imaging in two phases: early (10–20 minutes after tracer administration) and late (3–4 hours after). Image analysis includes the heart mediastinal ratio (H/M) for the quantification of global uptake, the washout rate (WR) to reflect catecholamine turnover and sympathetic activity and regional uptake on SPECT imaging. In HF patients, cardiac innervation is reduced, thus 123I-MIBG uptake is globally reduced.

H/M has emerged as one of the most powerful independent predictors of adverse cardiovascular events.[70,71] The AdreView Myocardial Imaging for Risk Evaluation in Heart Failure (ADMIRE-HF) trial,[72] a prospective multicentre study involving 961 patients, showed that a H/M <1.6 doubled the risk of HF progression, VT or cardiac death. More recently, a Japanese meta-analysis including 1,322 patients[73] proved that patients with H/M <1.68 or WR >43 % showed lower survival over a mean follow-up of 6.5 years. Other studies have evaluated 123I-MIBG imaging for the prediction of VT and SCD. In one of them, H/M resulted as an independent predictor for appropriate ICD therapy;[74] while in the other one WR correlated with higher SCD occurrence.[75] Moreover, studies consistently show that the H/R can reflect response to HF therapies, such as β-blockers[76] or LVADs,[77] as increases in H/R correlate with other clinical or analytical parameters.

Regional uptake assessment on SPECT adds relevant clinical information. Areas with autonomic tracer defect, but preserved perfusion tracer uptake (autonomic-perfusion mismatch), are more prone to develop lethal arrhythmias due to denervation supersensitivity.[78] The extent or severity of autonomic defects predicted VT inducibility[79] and occurrence of an ICD discharge or SCD.[80]

PET tracers such as 11C-hydroxyephedrine (11-CHED) improve the signal–noise ratio allowing better quantification.[81] The recent Prediction of Arrhythmic Events with Positron Emission Tomography (PAREPET) study[82] has proved that the extent of uptake defects correlated with the occurrence of SCD or ICD discharge.

Despite the increasing evidence, currently the assessment of cardiac innervation is not recommended as a routine test in the evaluation of HF patients. More studies are needed to define the subgroup of patients that could benefit most of this imaging technique.

Molecular Imaging

Molecular imaging techniques are emerging tools providing insight into disease manifestation before structural and physiological abnormalities become evident, although to date it has mainly been used for research purposes. A key factor in HF patients is myocardial remodelling. A multitude of cellular pathways implied in remodelling processes can be targeted: extracellular matrix degradation, angiogenesis, collagen deposition, etc.[83,84] Most tracers are still under development and have been only tested in animal models. Imaging myocardial activity of renin–angiotensin system seems to be a promising tool to monitor disease progression and medical therapy effectiveness in HF patients.[85]

Computed Tomography

Latest generation of multidetector CT (MDCT) allows obtaining high-quality images using a smaller amount of iodinated contrast.[86] In patients with HF, the increasing use of ICD-CRT devices, limits the

possibilities of performing a CMR. In this group of patients, MDCT emerges as a valid alternative to assess LV volumes and function.

Coronary Artery Disease

Evaluation of coronary calcium is a reliable test to discriminate ICM from NICM.[87] Coronary MDCT in patients with HF has a high negative predictive value to confirm in a non-invasive way the absence of CAD,[88–94] especially in new-onset HF patients. Taking into account the significance of CAD in HF patients, MDCT may be one of the most important non-invasive tests to perform in these patients. However, coronary MDCT provides anatomic but not physiological data on coronary disease, so no information about perfusion abnormalities can be extracted from it.

Due to the different attenuation characteristics of infarcted versus normal myocardium, measuring the infarct size is possible with MDCT. Those measurements have accurately correlated with those obtained on nuclear scanning and CMR.[95–98]

Cardiac Structure and Function

Several studies have shown excellent correlation between cardiac MDCT and other imaging modalities regarding diverse LV measurements: LVEF and global function, regional wall motion, wall thickness, chamber diameter, chamber volumes, stroke volume and cardiac output,[99–103] and provides adequate visualisation of RV wall thickness and function.[104,105] It can also obtain useful images to differentiate between some anatomic aetiologies of HF (for example, dilated versus hypertrophic cardiomyopathy). However, CMR is considered the gold standard for ventricular assessment and echocardiography is the most commonly used clinical test for this purpose.

Other Uses

MDCT can provide an accurate anatomic description of the pericardium (pericardial thickening, calcification, fatty infiltration and effusion), information of the anatomy of cardiac valves and assessment of ventricular contraction dyssynchrony, especially in those being assessed for CRT implantation.[106]

In cardiac transplantation, CT may obviate the need for routine invasive angiography to assess coronary allograft vasculopathy.[107,108]

Limitations and Contraindications of Computed Tomography

The two major risks with the procedure include contrast administration and radiation exposure. Cardiac CT cannot be performed in patients with contraindications to injection of iodinated contrast. Other relative contraindications include moderate to severe renal insufficiency and previous allergies to contrast. As for radiation, the effective radiation dose with 64-slice MDCT angiography is estimated to be approximately 11 to 22 mSv.

Hybrid Devices Computed Tomography Nuclear Image

Dual-image techniques offer the opportunity to use a single device for different purposes, such as determining perfusion, function and metabolism: adenosine stress CT myocardial perfusion imaging could detect haemodynamic significance of coronary stenosis detected by CT angiography.[109,110] Diverse combinations of hybrid imaging of myocardial perfusion (CT + SPECT, CT + PET and CT + CMR) are gaining increasing interest because they provide both anatomic and functional information, improving the overall performance of the diagnostic test.

Conclusion

There are several imaging modalities available for the evaluation of HF patients, each one with its highlights and pitfalls. Echocardiography continues to be the method of choice for its availability, cost and usefulness, it provides most of the information required for the management and follow up of HF patients and it has been enhanced with the development of 3DE and strain. Other non-invasive cardiac imaging modalities could provide additional aetiological, prognostic and therapeutic information, being helpful in making treatment decisions, especially in some subsets of patients (ischaemic heart disease, cardiomyopathies …) (see *Table 1*). An appropriate utilisation of imaging procedures should improve management and clinical outcomes in HF patients. ■

1. Kirkpatrick JN, Vannan MA, Narula J, et al. Echocardiography in heart failure: applications, utility, and new horizons. *J Am Coll Cardiol* 2007;**50**:381–96. PMID: 17662389
2. Foster E, Cahalan MK. The search for intelligent quantitation in echocardiography: "eyeball," "trackball" and beyond. *J Am Coll Cardiol* 1993;**22**:848–50. PMID: 8354822
3. Lang R, Badano L, Mor-Avi V, et al. Recommendations for cardiac chamber quantification by echocardiography in adults: An update from the American Society of Echocardiography and the European Association of Cardiovascular Imaging. *Eur Heart J Cardiovasc Imaging* 2015;**16**:233–71. doi: 10.1093/ehjci/jev014 PMID: 25712077
4. Morbach C, Lin B, Sugeng L., et al. Clinical application of three-dimensional echocardiography. *Prog Cardiovasc Dis* 2014;**57**:19–31. doi: 10.1016/j.pcad.2014.05.005 PMID: 25081399
5. Dorosz JL, Lezotte DC, Weitzenkamp DA, et al. Performance of 3-dimensional echocardiography in measuring left ventricular volumes and ejection fraction: a systematic review and meta-analysis. *J Am Coll Cardiol* 2012;**59**:1799–808. doi: 10.1016/j.jacc.2012.01.037 PMID: 22575319
6. Muraru D, Badano LP, Peluso D, et al. Comprehensive analysis of LV geometry and function by three-dimensional echocardiography in healthy adults. *J Am Soc Echocardiogr* 2013;**26**:618–28. doi: 10.1016/j.echo.2013.03.014 PMID: 23611056
7. Dalen H, Thorstensen A, Aase SA, et al. Segmental and global longitudinal strain and strain rate based on echocardiography of 1266 healthy individuals: the HUNT study in Norway. *Eur J Echocardiogr* 2010;**11**:176–83. doi: 10.1093/ejechocard/jep194 PMID: 19946115
8. Kocabay G, Muraru D, Peluso D, et al. Normal left ventricular mechanics by two-dimensional speckle tracking echocardiography. *Rev Esp Cardiol* 2014;**67**:651–8. doi: 10.1016/j.rec.2013.12.009 PMID: 25037544
9. Thavendiranathan P, Poulin F, Lim K, et al. Use of myocardial strain imaging by echocardiography for the early detection of cardiotoxicity in patients during and after cancer chemotherapy. *J Am Coll Cardiol* 2014;**63**:2751–68. doi: 10.1016/j.jacc.2014.01.073 PMID: 24703918
10. Buss SJ, Emami M, Mereles D, et al. Longitudinal left ventricular function for prediction of survival in systemic light-chain amyloidosis: incremental value compared with clinical and biochemical markers. *J Am Coll Cardiol* 2012;**60**:1067–76. doi: 10.1016/j.jacc.2012.04.043 PMID: 22883634
11. Phelan D, Collier P, Thavendiranathan P, et al. Relative apical sparing of longitudinal strain using two-dimensional speckle-tracking echocardiography is both sensitive and specific for the diagnosis of cardiac amyloidosis. *Heart* 2012;**98**:1442–8. doi: 10.1136/heartjnl-2012-302353 PMID: 22865865
12. Unzek S, Popovic ZB, Marwick TH. Effect of recommendations on inter-observer consistency of diastolic function evaluation: an international multicenter study. *JACC Cardiovasc Imaging* 2011;**4**:460–7. doi: 10.1016/j.jcmg.2011.01.016 PMID: 21565732
13. Mor-Avi V, Yodwut C, Jenkins C, et al. Real-time 3D echocardiographic quantification of left atrial volume: multicenter study for validation with CMR. *JACC Cardiovasc Imaging* 2012;**5**:769–77. doi: 10.1016/j.jcmg.2012.05.011 PMID: 22897989
14. Gibby C, Wiktor DM, Burgess M, et al. Quantitation of the diastolic stress test: filling pressure vs. diastolic reserve. *Eur Heart J Cardiovasc Imaging* 2013;**14**:223–7. doi: 10.1093/ehjci/jes078 PMID: 22729082
15. Holland DJ, Prasad SB, Marwick TH. Prognostic implications of left ventricular filling pressure with exercise. *Circ Cardiovasc Imaging* 2010;**3**:149–56. doi: 10.1161/CIRCIMAGING.109.908152 PMID: 20233862
16. Flachskampf F, Biering-Sørensen T, Solomon S, et al. Cardiac imaging to evaluate left ventricular diastolic function. *JACC Cardiovasc Imaging* 2015;**8**:1071–93. doi: 10.1016/j.jcmg.2015.07.004 PMID: 26381769
17. Wang J, Khoury DS, Thohan V, et al. Global diastolic stain rate for the assessment of left ventricular relaxation and filling pressures. *Circulation* 2007;**115**:1376–83. PMID: 17339549
18. Damy T, Goode KM, Kallvikbacka-Bennett A, et al. Determinants and prognostic value of pulmonary arterial pressure in patients with chronic heart failure. *Eur Heart J* 2010;**31**:2280–90. doi: 10.1093/eurheartj/ehq245 PMID: 20693169
19. Lu X, Nadvoretskiy V, Bu L, et al. Accuracy and reproducibility of real-time three-dimensional echocardiography for assessment of right ventricular volumes and ejection fraction in children. *J Am Soc Echocardiogr* 2008;**21**:84–9. PMID: 17628408
20. Maffessanti F, Gripari P, Tamborini G, et al. Evaluation of right ventricular systolic function after mitral valve repair: a two-dimensional Doppler, speckle-tracking, and three-dimensional echocardiographic study. *J Am Soc Echocardiogr* 2012;**25**:701–8. DOI: http://dx.doi.org/10.1016/j.echo.2012.03.017
21. Cameli M, Righini FM, Lisi M, et al. Comparison of right versus left ventricular strain analysis as a predictor of outcome in patients with systolic heart failure referred for heart transplantation. *Am J Cardiol* 2013;**112**:1778–84. doi: 10.1016/j.amjcard.2013.07.046 PMID: 24063825
22. Guendouz S, Rappeneau S, Nahum J, et al. Prognostic significance and normal values of 2D strain to assess right ventricular systolic function in chronic heart failure. *Circ J* 2012;**76**:127–36. PMID: 22033348
23. Pathan F, Marwick T. Myocardial Perfusion Imaging Using Contrast Echocardiography. *Prog Cardiovasc Dis* 2015;**57**:632–43. doi: 10.1016/j.pcad.2015.03.005 PMID: 25817740
24. Naji P, Griffin BP, Asfahan F, et al. Predictors of long-term outcomes in patients with significant myxomatous mitral regurgitation undergoing exercise echocardiography.

Circulation 2014;**129**:1310–9. doi: 10.1161/CIRCULATIONAHA.113.005287 PMID: 24396041
25. Desai MY, Bhonsale A, Patel P, et al. Exercise echocardiography in asymptomatic HCM. Exercise capacity, and not LV outflow tract gradient predicts long-term outcomes. *J Am Coll Cardiol Img* 2014;**7**:26–36. doi: 10.1016/j.jcmg.2013.08.010 PMID: 24290569
26. Chung ES, Leon AR, Tavazzi L, et al. Results of the Predictors of Response to CRT (PROSPECT) trial. *Circulation* 2008;**117**:2608–16. doi: 10.1161/CIRCULATIONAHA.107.743120 PMID: 18458170
27. Gorcsan J, Tayal B. Newer echocardiographic techniques in cardiac resynchronization therapy. *Card Electrophysiol Clin* 2015;**7**:609–18. doi: 10.1016/j.ccep.2015.08.013 PMID: 26596806
28. Stainback R, Estep J, Agler D, et al. Echocardiography in the management of patients with left ventricular assist devices: Recommendations from the American Society of Echocardiography. *J Am Soc Echocardiogr* 2015;**28**:853–909. doi: 10.1016/j.echo.2015.05.008 PMID: 26239899
29. Walsh TF, Hundley WG. Assessment of ventricular function with cardiovascular magnetic resonance. *Cardiol Clin* 2007;**25**:15–33. PMID: 17478238
30. Karamitsos TD, Francis JM, Myerson S, et al. The role of cardiovascular magnetic resonance imaging in heart failure. *J Am Coll Cardiol* 2009;**54**:1407–24. doi: 10.1016/j.jacc.2009.04.094 PMID: 19796734
31. McCrohon JA, Moon JC, Prasad SK, et al. Differentiation of heart failure related to dilated cardiomyopathy and coronary artery disease using gadolinium-enhanced cardiovascular magnetic resonance. *Circulation* 2003;**108**:54–9. PMID: 12821550
32. Soriano CJ, Ridocci F, Estornell J, et al. Noninvasive diagnosis of coronary artery disease in patients with heart failure and systolic dysfunction of uncertain etiology, using late gadolinium-enhanced cardiovascular magnetic resonance. *J Am Coll Cardiol* 2005;**45**:743–8. doi:10.1016/j.jacc.2004.11.037
33. Assomull RG, Shakespeare C, Kalra PR, et al. Role of cardiovascular magnetic resonance as a gatekeeper to invasive coronary angiography in patients presenting with heart failure of unknown etiology. *Circulation* 2011;**124**:1351–60. doi: 10.1161/CIRCULATIONAHA.110.011346 PMID: 21900085
34. Heydari B, Jerosch-Herold M, Kwong RY. Assessment of myocardial ischemia with cardiovascular magnetic resonance. *Prog Cardiovasc Dis* 2011;**54**:191–203. doi: 10.1016/j.pcad.2011.09.004 PMID: 22014487
35. Roberts WC, Siegel RJ, McManus BM. Idiopathic dilated cardiomyopathy: analysis of 152 necropsy patients. *Am J Cardiol* 1987;**60**:1340–55. PMID: 3687784
36. Greenwood JP, Maredia N, Younger JF, et al. Cardiovascular magnetic resonance and single-photon emission computed tomography for diagnosis of coronary heart disease (CE-MARC): a prospective trial. *Lancet* 2012;**379**:453–60. doi: 10.1016/S0140-6736(11)61335-4 PMID: 22196944
37. Bruder O, Schneider S, Nothnagel D, et al. EuroCMR (European Cardiovascular Magnetic Resonance) registry: results of the German pilot phase. *J Am Coll Cardiol* 2009;**54**:1457–66. doi: 10.1016/j.jacc.2009.07.003 PMID: 19682818
38. Selvanayagam JB, Kardos A, Francis JM, et al. Value of delayed-enhancement cardiovascular magnetic resonance imaging in predicting myocardial viability after surgical revascularization. *Circulation* 2004;**110**:1535–41. PMID: 15353496
39. Kim RJ, Wu E, Rafael A, et al. The use of contrast-enhanced magnetic resonance imaging to identify reversible myocardial dysfunction. *N Engl J Med* 2000;**343**:1445–53. PMID: 11078769
40. Bonow RO, Maurer G, Lee KL, et al. Myocardial viability and survival in ischemic left ventricular dysfunction. *N Engl J Med* 2011;**364**:1617–25. doi: 10.1056/NEJMoa1100358 PMID: 21463153
41. Gerber BL, Rousseau MF, Ahn SA, et al. Prognostic value of myocardial viability by delayed-enhanced magnetic resonance in patients with coronary artery disease and low ejection fraction: impact of revascularization therapy. *J Am Coll Cardiol* 2012;**59**:825–35. doi: 10.1016/j.jacc.2011.09.073 PMID: 22361403
42. Arai AE. The cardiac magnetic resonance (CMR) approach to assessing myocardial viability. *J Nucl Cardiol* 2011;**18**:1095–102. doi: 10.1007/s12350-011-9441-5 PMID: 21882082
43. Wu KC. CMR of microvascular obstruction and hemorrhage in myocardial infarction. *J Cardiovasc Magn Reson* 2012;**14**:68. doi:10.1186/1532-429X-14-68 PMID: 23021401
44. Wu KC, Zerhouni EA, Judd RM, et al. Prognostic significance of microvascular obstruction by magnetic resonance imaging in patients with acute myocardial infarction. *Circulation* 1998;**97**:765–72. PMID: 9498540
45. Nijveldt R, Beek AM, Hirsch A, et al. Functional recovery after acute myocardial infarction: comparison between angiography, electrocardiography, and cardiovascular magnetic resonance measures of microvascular injury. *J Am Coll Cardiol* 2008;**52**:181–9. doi: 10.1016/j.jacc.2008.04.006 PMID: 18617066
46. Bleeker GB, Kaandorp TA, Lamb HJ, et al. Effect of posterolateral scar tissue on clinical and echocardiographic improvement after cardiac resynchronization therapy. *Circulation* 2006;**113**:969–76. PMID: 16476852
47. White JA, Yee R, Yuan X, et al. Delayed enhancement magnetic resonance imaging predicts response to cardiac resynchronization therapy in patients with intraventricular dyssynchrony. *J Am Coll Cardiol* 2006;**48**:1953–60. PMID: 17112984
48. Leyva F, Foley PW, Chalil S, et al. Cardiac resynchronization therapy guided by late gadolinium-enhancement cardiovascular magnetic resonance. *J Cardiovasc Magn Reson* 2011;**13**:29. doi: 10.1186/1532-429X-13-29 PMID: 21668964
49. Gao P, Yee R, Gula L, et al. Prediction of arrhythmic events in ischemic and dilated cardiomyopathy patients referred for implantable cardiac defibrillator: evaluation of multiple scar quantification measures for late gadolinium enhancement magnetic resonance imaging. *Circ Cardiovasc Imaging* 2012;**5**:448–56. doi: 10.1161/CIRCIMAGING.111.971549 PMID: 22572740
50. Ugander M, Oki AJ, Hsu LY, Kellman P, et al. Extracellular volume imaging by magnetic resonance imaging provides insights into overt and sub-clinical myocardial pathology. *Eur Heart J* 2012;**33**:1268–78. doi: 10.1093/eurheartj/ehr481 PMID: 22279111
51. Mahrholdt H, Wagner A, Deluigi CC, et al. Presentation, patterns of myocardial damage, and clinical course of viral myocarditis. *Circulation* 2006;**114**:1581–90. PMID: 17015795
52. De Cobelli F, Pieroni M, Esposito A, et al. Delayed gadolinium-enhanced cardiac magnetic resonance in patients with chronic myocarditis presenting with heart failure or recurrent arrhythmias. *J Am Coll Cardiol* 2006;**47**:1649–54. PMID: 16631005
53. Klopotowski M, Kukula K, Malek LA, et al. The value of cardiac magnetic resonance and distribution of late gadolinium enhancement for risk stratification of sudden cardiac death in patients with hypertrophic cardiomyopathy. *J Cardiol* 2015: epub ahead of print. doi: 10.1016/j.jjcc.2015.07.020 PMID: 26363820
54. Ismail TF, Jabbour A, Gulati A, et al. Role of late gadolinium enhancement cardiovascular magnetic resonance in the risk stratification of hypertrophic cardiomyopathy. *Heart* 2014;**100**:1851–8. doi: 10.1136/heartjnl-2013-305471 PMID: 24966307
55. Cheng AS, Banning AP, Mitchell AR, et al. Cardiac changes in systemic amyloidosis: visualisation by magnetic resonance imaging. *Int J Cardiol* 2006;**113**:E21–3. PMID: 17049635
56. Hendel RC, Berman DS, Di Carli MF, et al. ACCF/ASNC/ACR/AHA/ASE/SCCT/SCMR/SNM 2009 appropriate use criteria for cardiac radionuclide imaging: a report of the American College of Cardiology Foundation Appropriate Use Criteria Task Force, the American Society of Nuclear Cardiology, the American College of Radiology, the American Heart Association, the American Society of Echocardiography, the Society of Cardiovascular Computed Tomography, the Society for Cardiovascular Magnetic Resonance, and the Society of Nuclear Medicine. *Circulation* 2009;*119*:e561–87. doi: 10.1161/CIRCULATIONAHA.109.192519 PMID: 19451357
57. Udelson JE, Shafer CD, Carrió I. Radionuclide imaging in hear failure: Assessing etiology and outcomes and implications for management. *J Nucl Cardiol* 2002;**9**:S40–S52. PMID: 12271264
58. Danias PG, Papaioannou GI, Ahlberg AW, et al. Usefulness of electrocardiographic-gatedstress technetium-99m sestamibi single-photon emission computed tomography to differentiate ischemic from nonischemic cardiomyopathy. *Am J Cardiol* 2004;**94**:14–9. PMID: 15219501
59. Candell-Riera J, Romero-Farina G, Aguade-Bruix S, et al. Prognostic value of myocardial perfusion gated SPECT in patients with ischemic cardiomyopathy. *J Nucl Cardiol* 2009;**16**:212–21. doi: 10.1007/s12350-008-9042-0 PMID: 19159990
60. Tio RA, Dabeshlim A, Siebelink HM, et al. Comparison between the prognostic value of left ventricular function and myocardial perfusion reserve in patients with ischemic heart disease. *J Nucl Med* 2009;**50**:214–9. doi: 10.2967/jnumed.108.054395 PMID: 19164219
61. Di Carli MF, Dorbala S, Meserve J, et al. Clinical myocardial perfusion PET/CT. *J Nucl Med* 2007;**48**:783–93. PMID: 17475968
62. Camici PG, Crea F. Coronary microvascular dysfunction. *N Engl J Med* 2007;356:830–40. PMID: 17314342
63. Neglia D, Michelassi C, Trivieri MG, et al. Prognostic role of myocardial blood flow impairment in idiopathic left ventricular dysfunction. *Circulation* 2002;**105**:186–93.
64. Partington SL, Kwong RY, Dorbala S. Multimodality imaging in the assessment of myocardial viability. *Heart Fail Rev* 2011;**16**:381–95. doi: 10.1007/s10741-010-9201-7 PMID: 21069458 PMCID: PMC3954520
65. Marcassa C, Galli M, Cuocolo A, et al. Rest-redistribution thallium-201 and rest technetium-99m-sestamibi SPECT in patients with stable coronary artery disease and ventricular dysfunction. *J Nucl Med* 1997;**38**:419–24. PMID: 9074530
66. Schinkel AF, Bax JJ, Poldermans D, et al. Hibernating myocardium: Diagnosis and patient outcomes. *Curr Probl Cardiol* 2007;**32**:375–410. PMID: 17560992
67. D'Egidio G, Nichol G, Williams KA, et al. Increasing benefit from revascularization is associated with increasing amounts of myocardial hibernation: A substudy of thePARR-2 trial. *JACC Cardiovasc Imaging* 2009;**2**:1060–8. doi: 10.1016/j.jcmg.2009.02.017 PMID: 19761983
68. Inaba Y, Chen JA, Bergmann SR. Quantity of viable myocardium required to improve survival with revascularization in patients with ischemic cardiomyopathy: A meta-analysis. *J Nucl Cardiol* 2010;**17**:646–54. doi: 10.1007/s12350-010-9226-2 PMID: 20379861
69. Langer O, Halldin C. PET and SPET tracers for mapping the cardiac nervous system. *Eur J Nucl Med Mol Imaging* 2002;**29**:416–34. PMID: 12002720
70. Agostini D, Verberne HJ, Burchert W, et al. I-123-mIBG myocardial imaging for assessment of risk for a major cardiac event in heart failure patients: Insights from a retrospective European multicenter study. *Eur J Nucl Med Mol Imaging* 2008;**35**:535–46. PMID: 18043919
71. Manrique A, Bernard M, Hitzel A, et al. Prognostic value of sympathetic innervation and cardiac asynchrony in dilated cardiomyopathy. *Eur J Nucl Med Mol Imaging* 2008;**35**:2074–81. doi: 10.1007/s00259-008-0889-8 PMID: 18682936
72. Jacobson AF, Senior R, Cerqueira MD, et al. Myocardial iodine-123 meta-iodobenzylguanidine imaging and cardiac events in heart failure. Results of the prospective ADMIRE-HF (AdreView Myocardial Imaging for Risk Evaluation in Heart Failure) study. *J Am Coll Cardiol* 2010;**55**:2212–21. doi: 10.1016/j.jacc.2010.01.014 PMID: 20188504
73. Nakata T, Nakajima K, Yamashina S, et al. A pooled analysis of multicenter cohort studies of I-123-mIBG cardiac sympathetic innerva- tion imaging for assessment of long-term prognosis in chronic heart failure. *J Am Coll Cardiol Imaging* 2013;**6**:772–84. doi: 10.1016/j.jcmg.2013.02.007 PMID: 23845574
74. Nagahara D, Nakata T, Hashimoto A, et al. Predicting the need for an implantable cardioverter defibrillator using cardiac metaiodobenzylguanidine activity together with plasma natriuretic peptide concentration or left ventricular function. *J Nucl Med* 2008;**49**:225–33. doi: 10.2967/jnumed.107.042564 PMID: 18199625
75. Kioka H, Yamada T,Mine T, et al. Prediction of sudden death in patients with mild-to-moderate chronic heart failure by using cardiac iodine-123 metaiodobenzylguanidine imaging. *Heart* 2007;**93**:1213–8. PMID: 17344327
76. Treglia G, Stefanelli I, Giordano BA. Clinical usefulness of myocardial innervation imaging using Iodine-123-meta-iodobenzylguanidine scintigraphy in evaluating the effectiveness of pharmacological treatments in patients with heart failure: An overview. *Eur Rev Med Pharmacol Sci* 2013;**17**:56–8.
77. George RS, Birks EJ, Cheetham A, et al. The effect of long-term left ventricular assist device support on myocardial sympathetic activity in patients with non-ischaemic dilated cardiomyopathy. *Eur J Heart Fail* 2013;**15**:1035–43. doi: 10.1093/eurjhf/hft059 PMID: 23610136
78. Simões MV, Barthel P, Matsunari I, et al. Presence of sympathetically denervated but viable myocardium and its electrophysiologic correlates after early revascularised, acute myocardial infarction. *Eur Heart J* 2004;**25**:551–7. PMID: 15120051
79. Bax JJ, Kraft O, Buxton AE, et al. 123I-mIBG Scintigraphy to predict inducibility of ventricular arrhythmias on cardiac electrophysiology testing: A prospective multicenter pilot study. *Circ Cardiovasc Imaging* 2008;**1**:131–40. doi: 10.1161/CIRCIMAGING.108.782433 PMID: 19808530
80. Boogers MJ, Borleffs CJ, Henneman MM, et al. Cardiac sympathetic denervation assessed with 123-Iodine metaiodobenzylguanidine imaging predicts ventricular arrhythmias in implantable cardioverter-defibrillator patients. *J Am Coll Cardiol* 2010;**55**:2769–77. doi: 10.1016/j.jacc.2009.12.066 PMID: 20538172
81. Luisi AJ Jr, Suzuki G, Dekemp R, et al. Regional 11C-Hydroxyephedrine retention in hibernating myocardium: Chronic inhomogeneity of sympathetic innervation in the absence of infarction. *J Nucl Med* 2005;**46**:1368–74. PMID: 16085596
82. Fallavollita JA, Canty JM. Dysinnervated but viable myocardium in ischemic heartdisease, *J Nucl Cardiol* 2010;**17**:1107–15. doi: 10.1007/s12350-010-9292-5 PMID: 20857351 PMCID: PMC3026632
83. Chen IY, Wu JC. Cardiovascular molecular imaging: focus on clinical translation. *Circulation* 2011;**123**:425–43. doi: 10.1161/CIRCULATIONAHA.109.916338 PMID: 21282520 [PubMed - indexed for MEDLINE] PMCID: PMC3073678
84. Kramer CM, Sinusas AJ, Sosnovik DE, et al. Multimodality imaging of myocardial injury and remodeling. *J Nucl Med* 2010;**51**:107S–121S. doi: 10.2967/jnumed.109.068221 PMID: 20395347 [PubMed - indexed for MEDLINE] PMCID: PMC3078824
85. Fukushima K, Bravo PE, Higuchi T, et al. Molecular hybrid positron emission tomography/computed tomography imaging of cardiac angiotensin II type 1 receptors. *J Am Coll Cardiol* 2012;**60**:2527–34. doi: 10.1016/j.jacc.2012.09.023 PMID: 23158533 [PubMed - indexed for MEDLINE] PMCID: PMC3522758
86. Butler J. The emerging role of multi-detector computed tomography in heart failure. *J Card Fail* 2007;**13**:215–26. PMID: 17448420
87. Shemesh J, Tenenbaum A, Fisman EZ, et al. Coronary calcium as a reliable tool for differentiating ischemic from nonischemic cardiomyopathy. *Am J Cardiol* 1996;**77**:191–4. PMID: 8546091
88. Andreini D, Pontone G, Pepi M, et al. Diagnostic accuracy of multidetector computed tomography coronary angiography in patients with dilated cardiomyopathy. *J Am Coll Cardiol* 2007;**49**:2044–50. PMID: 17512361
89. Cornily JC, Gilard M, Le Gal G, et al. Accuracy of 16-detector multislice spiral computed tomography in the initial evaluation of dilated cardiomyopathy. *Eur J Radiol* 2007;**61**:84–

90. PMID: 16987628
90. Nielsen LH, Olsen J, Markenvard J, et al. Effects on costs of frontline diagnostic evaluation in patients suspected of angina: coronary computed tomography angiography vs. conventional ischaemia testing. *Eur Heart J Cardiovasc Imaging* 2013;**14**:449–55.
91. D'Ascenzo F, Cerrato E, Biondi–Zoccai G, et al. Coronary computed tomographic angiography for detection of coronary artery disease in patients presenting to the emergency department with chest pain: a meta-analysis of randomized clinical trials. *Eur Heart J Cardiovasc Imaging* 2013;**14**:782–9. doi: 10.1093/ehjci/jes287 PMID: 23221314
92. Hulten E, Pickett C, Bittencourt MS, et al. Meta-analysis of coronary CT angiography in the emergency department. *Eur Heart J Cardiovasc Imaging* 2013;**14**:607. doi: 10.1093/ehjci/jet027 PMID: 23460725
93. Gebhard C, Fiechter M, Fuchs TA, et al. Coronary artery stents: influence of adaptive statistical iterative reconstruction on image quality using 64-HDCT. *Eur Heart J Cardiovasc Imaging* 2013;**14**:969–77. doi: 10.1093/ehjci/jet013 PMID: 23428650 PMID: 23360870
94. Rubinshtein R, Gaspar T, Lewis BS, et al. Long-term prognosis and outcome in patients with a chest pain syndrome and myocardial bridging: a 64-slice coronary computed tomography angiography study. *Eur Heart J Cardiovasc Imaging* 2013;**14**:579–85. doi: 10.1093/ehjci/jet010
95. Baks T, Cademartiri F, Moelker AD, et al. Multislice computed tomography and magnetic resonance imaging for the assessment of reperfused acute myocardial infarction. *J Am Coll Cardiol* 2006;48:144e52. PMID: 16814660
96. Kim RJ, Wu E, Rafael A, et al. The use of contrast-enhanced magnetic resonance imaging to identify reversible myocardial dysfunction. *N Engl J Med* 2000;**343**:1445e53. PMID: 11078769
97. Mendoza DD, Joshi SB, Weissman G, et al. Viability imaging by cardiac computed tomography. *J Cardiovasc Comput Tomogr* 2010;**4**:83–91. doi: 10.1016/j.jcct.2010.01.019 PMID: 20430338
98. Le Polain de Waroux JB, Pouleur AC, Goffinet C, et al. Combined coronary and late-enhanced multidetector-computed tomography for delineation of the etiology of left ventricular dysfunction: comparison with coronary angiography and contrast-enhanced cardiac magnetic resonance imaging. *Eur Heart J* 2008;**29**:2544–51. doi: 10.1093/eurheartj/ehn381 PMID: 18762553
99. Juergens KU, Grude M, Maintz D, et al. Multi-detector row CT of left ventricular function with dedicated analysis software versus MR imaging: initial experience. *Radiology* 2004;**230**:403e10. PMID: 14668428
100. Mahnken AH, Koos R, Katoh M, et al. Sixteen-slice spiral CT versus MR imaging for the assessment of left ventricular function in acute myocardial infarction. *EurRadiol* 2005;**15**:714e20. PMID: 14668428
101. Dewey M, Muller M, Teige F, Hamm B. Evaluation of a semiautomatic software tool for left ventricular function analysis with 16-slice computed tomography. *EurRadiol* 2006;**16**:25e31. PMID: 15965660
102. Heuschmid M, Rothfuss JK, Schroeder S, et al. Assessment of left ventricular function using 16-slice multidetector-row computed tomography: comparison with MRI and echocardiography. *EurRadiol* 2006;**16**:551e9. PMID: 16215736
103. Butler J, Shapiro MD, Jassal DS, et al. Comparison of multidetector computed tomography and two-dimensional transthoracic echocardiography for left ventricular assessment in patients with heart failure. *Am J Cardiol* 2007;**99**:247–9.
104. Dogan H, Kroft LJ, Bax JJ, et al. MDCT assessment of right ventricular systolic function. *Am J Roentgenol* 2006;**186**:S366e70. PMID: 16714610
105. Kim TH, Ryu YH, Hur J, et al. Evaluation of right ventricular volume and mass using retrospective ECG-gated cardiac MDCT: comparison with first-pass radionuclide angiography. *EurRadiol* 2005;**5**:1987e93. PMID: 15776241
106. Leclercq C, Kass DA. Retiming the failing heart: principles and current clinical status of cardiac resynchronization. *J Am Coll Cardiol* 2002;**39**:194e201. PMID: 11788207
107. Taylor DO, Edwards LB, Boucek MM, et al. The Registry of the International Society for Heart and Lung Transplantation: twenty-first official adult heart transplant reportd2004. *J Heart Lung Transplant* 2004;**23**:796e803. PMID: 15285065
108. Sigurdsson G, Carrascosa P, Yamani MH, et al. Detection of transplant coronary artery disease using multidetector computed tomography with adaptative multisegment reconstruction. *J Am Coll Cardiol* 2006;**48**:772–8. PMID: 16904548
109. Rossi A, Uitterdijk A, Dijkshoorn M, et al. Quantification of myocardial blood flow by adenosine-stress CT perfusion imaging in pigs during various degrees of stenosis correlates well with coronary artery blood flow and fractional flow reserve. *Eur Heart J Cardiovasc Imaging* 2013;**14**:331–8. doi: 10.1093/ehjci/jes150 PMID: 22843541
110. Schaap J, Kauling RM, Boekholdt SM, et al. Incremental diagnostic accuracy of hybrid SPECT/CT coronary angiography in a population with an intermediate to high pre-test likelihood of coronary artery disease. *Eur Heart J Cardiovasc Imaging* 2013;**14**:642–9. doi: 10.1093/ehjci/jes303 PMID: 23291392